Ethanol-Assisted Dispersion of Attapulgite and Its Effect on Improving Properties of Alginate-Based Superabsorbent Nanocomposite

Yizhe Wang,[1,2] Xiaoning Shi,[1,2] Wenbo Wang,[1,3] Aiqin Wang[1,3]

[1]Center of Eco-material and Green Chemistry, Lanzhou Institute of Chemical Physics, Chinese Academy of Sciences, Lanzhou 730000, People's Republic of China
[2]Graduate University of the Chinese Academy of Sciences, Beijing 100049, People's Republic of China
[3]R&D Center of Xuyi Attapulgite Applied Technology, Lanzhou Institute of Chemical Physics, Chinese Academy of Science, Xuyi, 211700, People's Republic of China
Correspondence to: A. Wang (E-mail: aqwang@licp.cas.cn)

ABSTRACT: The dispersion of attapulgite (APT) as nanorod-like single crystals is crucial to fully develop its functionality of one-dimensional nanometer material as a filler of composite materials. In this study, APT was dispersed by the assistance of ethanol during the high-pressure homogenization process to form individual nanorod-like crystals. The dispersed APT was used to prepare new sodium alginate-g-poly(sodium acrylate-co-styrene)/attapulgite (NaAlg-g-P(NaA-co-St)/APT) superabsorbent nanocomposites. The effect of ethanol/water ratio on the dispersion of crystal bundles of APT was investigated by field emission scanning electron microscopy, and the results indicate that APT crystal bundles were effectively disaggregated in $v(CH_3CH_2OH) : v(H_2O) - 5 : 5$ solution after homogenized at 50 MPa. The better dispersion of APT in NaAlg-g-P(NaA-co-St) matrix has clearly improved the gel strength (from 1300 Pa to 1410 Pa, $\omega = 100$ rad/s), swelling capacity (442–521 g/g), swelling rate (3.3303–4.5736 g/g/s), and reswelling ability of the superabsorbent nanocomposite. Moreover, the nanocomposites showed fast swelling–deswelling responsive behavior in different saline solutions. © 2012 Wiley Periodicals, Inc. J. Appl. Polym. Sci. 129: 1080–1088, 2013

INTRODUCTION

Superabsorbent materials have raised great attention owing to their excellent water absorbent and retention properties, which have found potential application in many fields, such as agriculture,[1] hygienic products,[2] wastewater treatment,[3,4] drug delivery,[5,6] and so on. Recently, the organic inorganic nanocomposites based on natural polymers and silicate clays have been focused because the resultant superabsorbent materials combined the renewable, nontoxic, and biodegradable characteristics of natural polymers as well as the abundant, low-cost, heat-resistant, and reinforce advantages of inorganic nanoclays.[7,8] Thus far, many natural polymers (e.g., starch,[9,10] cellulose,[11,12] chitosan,[13] guar gum,[14] alginate,[15] carrageenin,[16] etc.) and various clays (e.g., kaolin,[17] mica,[18] vermiculite,[19] attapulgite (APT),[20] montmorillonite,[21] rectorite,[22] medicinal stone,[23] etc.) have been used, and the introduction of these clays into the natural polymer-based superabsorbents can not only improve their gel strength, swelling ability, swelling rate, and salt resistance, but also reduce the production cost,[24] and it was confirmed that the dispersion of nanoclays is responsible for the performance of the composite materials.

Sodium alginate (NaAlg) is an anionic natural polymer composed of α-1,4-L-glucuronic acid (G units) and poly-β-1,4-D-mannuronic acid (M units) in varying proportions by 1-4 linkages. NaAlg can be extracted from marine algae or produced by bacteria, and hence it is abundant, renewable, nontoxic, water soluble, biodegradable, and biocompatible. In addition, NaAlg can be easily modified through grafting copolymerization or compounding with clay to derive superabsorbent materials with higher water absorption capacity.[25]

APT is a natural hydrated magnesium aluminum silicate containing ribbons of a 2 : 1 phyllosilicate structure. The reactive —OH group on the surface of APT endows it with better reaction activity, and hence APT is convenient to participate in grafting polymerization with hydrophilic vinyl monomers. In addition, the one-dimensional nanoscale rod structure makes APT, having better reinforce performance as a filler of

composite material. Thus, APT was considered as a promising candidate to prepare superabsorbent nanocomposites.[26] In the previous study of our group, it was found that the suitable pre-treatment of APT nanoparticle renders it more compatible with the organic matrix and better dispersion in the nanocomposite.[27–29] For this reason, the incorporation of modified APT can improve the properties of superabsorbents to a higher degree than the raw ones. Currently, the common modification methods for APT are ion-exchange, organification, acidification, and heat activation treatment.[27–29] However, these methods can not efficiently disaggregate the APT crystal bundles as expected. Our latest research showed that high-pressure homogenization technology could disperse APT crystal bundles effectively by the cavity effect, which overwhelms the interactions among the fibrous crystals.[30] In addition, it is well known that ethanol solution is often used as dispersed medium in many applications.[31,32] Thus, it is expected that the usage of ethanol during high-pressure homogenization process could disperse APT crystal bundles into nanoscale rod crystal, and the gel strength and swelling properties of the superabsorbent can be improved by the dispersion of APT. But, to the best of our knowledge, rare research regards to the effect of APT dispersion by ethanol on the properties of superabsorbent.

On the basis of our previous study about sodium alginate-based superabsorbents,[33] the APT clays treated with different ethanol/water ratio via high-pressure homogenization process were introduced to prepare the sodium alginate-g-poly(sodium acrylate-co-styrene)/attapulgite (NaAlg-g-P(NaA-co-St)/APT) superabsorbent nanocomposites. The chemical structures and surface morphology of the nanocomposites were confirmed by field emission scanning electron microscopy (FESEM) and Fourier transform infrared spectroscopy (FTIR). The influence of the ethanol/water treatment for APT on the gel strength, water absorbency, swelling rate, reswelling ability, and other swelling properties was investigated in detail.

EXPERIMENTAL

Materials

NaAlg was purchased from Shanghai Chemical Reagents (Shanghai, China). APT, obtained from Jiuchuan Technology, (Jiangsu, China), is composed of 1.29% CaO, 10.47% Al_2O_3, 1.52% Na_2O, 20.41% MgO, 64.31% SiO_2, 0.13% K_2O, and 0.87% Fe_2O_3 as determined by X-ray fluorescence spectrometer (Minipal 4, PANalytical, Almelo, The Netherlands). Acrylic acid (AA, chemical pure, Shanghai Shanpu Chemical Factory, Shanghai, China) was distilled under reduced pressure before use. Styrene (St, chemical pure, Shantou Xilong Chemical Factory, Shantou, China), Ammonium persulfate (APS, analytical grade, Tianjin Chemical Reagent, Tianjin, China) and N,N'-methylenebisacrylamide (MBA, chemical pure, Shanghai Yuanfan Auxiliaries, Shanghai, China) were used as received. The other reagents used were all of analytical grade, and all solutions were prepared with deionized water.

Ethanol-Assisted Dispersion of APT via High-Pressure Homogenization

In brief, 50.0 g of APT was dispersed in 500 mL of various dispersed media ($v(CH_3CH_2OH)$: $v(H_2O)$ - 0 : 10, 2 : 8, 4 : 6, 5 : 5, 6 : 4, 8 : 2, and 10 : 0, respectively) and mechanically stirred

at 800 rpm for 120 min to obtain a homogeneous suspension. The obtained suspension was filtered through a vibrating sieve to remove quartz and other impurities. Subsequently, the collected APT suspension was homogenized with a high-pressure homogenizer (GYB-3004, Shanghai Donghua High-Pressure Homogenizer Factory, Shanghai, China) at 50 MPa. The homogenized suspensions were centrifuged at 5000 rpm for 20 min, and the solid products were dried at 105°C for 4 h. Finally, the dry products were grounded and passed through a 200-mesh screen. The sample dispersed in water and prepared according to the similar procedure without homogenization treatment was also obtained to compare the effect of a homogenization process on dispersion properties of APT. All APT samples with a particle size smaller than 74 μm were used for further experiments.

Synthesis of NaAlg-g-P(NaA-co-St)/APT Superabsorbent Nanocomposites

NaAlg (1.20 g) was dissolved in 30 mL distilled water in a 250-mL four-necked flask equipped with a mechanical stirrer, a reflux condenser, a thermometer, and a nitrogen line. The reactor was immersed in an oil bath at 60°C and kept for 1 h, at the same time, purged with nitrogen to remove the oxygen dissolved in the system. Then, APS (0.100 g, dissolved in 5 mL distilled water) was added to the slurry, and the reaction mixture was stirred continuously (250 rpm) at 60°C for 15 min. Then, the reactants were cooled to 40°C, and the mixture of AA (7.2 g, partially neutralized by 8.8 mL 8M NaOH solution), St (0.1439 g), and APT (0.928 g) was added. Keeping the mixture stirred for 10 min, MBA (0.018 g) was added. Again, the oil bath was slowly heated to 70°C and maintained for 3 h to complete the polymerization. Finally, the obtained gel products were dried in an oven at 70°C for 72 h. All the samples were passed through 40 80 mesh sieve (180 380 μm) after ground.

Determination of Gel Strength

The gel strength of the superabsorbent nanocomposite at swelling state was measured on a Physica MCR 301 rheometer (Germany) by a rheological method developed previously.[34] Typically, the dry sample was swelled in distilled water to a swelling ratio of 100 g/g. The storage modulus (G') was determined using parallel plates of 25 mm diameter at 25° and the rheological curves of storage modulus (Pa) versus angular frequency (ω, rad/s) were recorded. The constant deformation strain of 0.5% was used, and the angular frequency ω was defined in the range of 0.1–100 rad/s. The reported results are the average of at least three measurements.

Measurements of Equilibrium Water Absorbency and Swelling Kinetic

To determine the equilibrium water absorbency of the superabsorbents, dried sample of 0.050 g was immersed in 200 mL distilled water or other swelling media at room temperature for 3 h to reach swelling equilibrium. The swollen gels were filtrated from the unabsorbed water by a 100-mesh sieve and drained for 10 min until no residual free water. The equilibrium water absorbency (Q_{eq}, g/g) was calculated by eq. (1).

$$Q_{eq} = (M_s - M_d)/M_d \qquad (1)$$

Here, M_d and M_s are the masses of dried sample (g) and swollen hydrogel (g), respectively. Each measurement was repeated

for three times to obtain a mean value of Q_{eq} and the $\pm$SD range is <3%.

Swelling kinetics of the superabsorbents was measured as follows: sample of 0.050 g was soaked in 200 mL solution. The swollen gels were filtered out using a sieve at the consecutive time intervals (1, 3, 5, 7, 10, 15, 20, 30, 60, and 120 min, respectively), the swelling capacity (Q_t) of the superabsorbents at a given time t was measured by weighing the swollen (M_{st}) and the dry (M_d) samples and was calculated according to eq. (1).

Deswelling kinetics of the swollen hydrogels in different saline solutions (15 mmol/L) was also measured as above. The fully swollen hydrogels were soaked in 200 mL saline solution for different time intervals, and then the hydrogels were separated from the saline solution and weighed. The amount of water retention (WR) by the hydrogel network at a time moment was calculated by the following equation:

$$WR - (M_t - M_d)/M_s \times 100 \qquad (2)$$

where M_t is the mass of hydrogel deswelling at time t, M_d and M_s are the masses of gel at dry state and swelling state, respectively.

Reswelling Capability

The sample (0.05 g) was soaked in 100 mL of distilled water to achieve the swelling equilibrium, and then the swollen sample was placed in an oven to dehydrate at 100°C. After dried thoroughly, the equal volume of water was added to the recovered superabsorbent to reach swelling equilibrium. The swollen samples were dehydrated by above procedure again. Similar procedure was repeated for several times to evaluate the reswelling capability of the superabsorbents.

Characterizations

The FTIR spectra were recorded on a Nicolet NEXUS FTIR spectrometer in the range of 4000–400 cm[1] region using KBr pellets. The morphologies of the samples were examined using a JSM-6701F Field Emission Scanning Electron Microscope (JEOL) after coating the sample with gold film.

RESULTS AND DISCUSSION

FTIR Spectra Analysis

The FTIR spectra of the different ratio of ethanol/water-treated APT and the corresponding superabsorbent nanocomposites are shown in Figure 1. As it can be observed [Figure 1(a, c)], the characteristic absorption bands of APT at 3420–3614, 1654, 1197, 1030, and 982 cm[1] have no obvious change after dispersed with different volume ratios of ethanol/water solutions. This reveals that the treatment process of APT can only disaggregate APT fibrous bundles and will not alter chemical structures of APT. As shown in Figure 1(e, f), the FTIR spectra of the superabsorbent nanocomposites also made no difference as expected. The Si─OH stretching vibration of APT at 3551 cm[1] disappeared, indicating that the APT took part in the graft polymerization by the ─OH groups on the surface of clay. The absorption band at 1738 cm[1] was ascribed to the C─O asymmetric stretching vibration and the peaks at 1632, 1458, and 1404 cm[1] were owing to the asymmetric
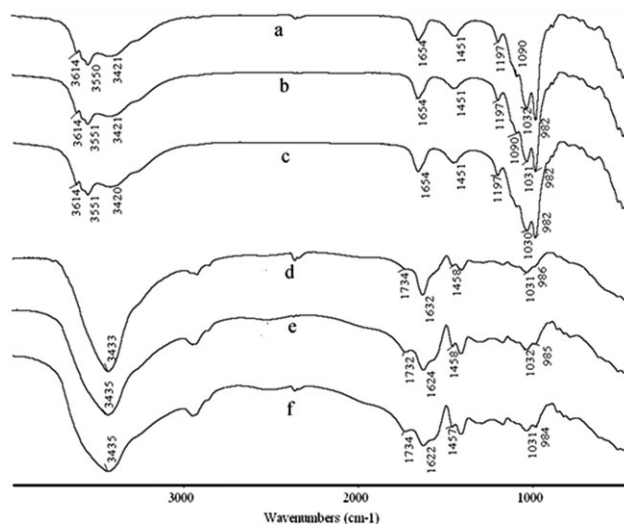
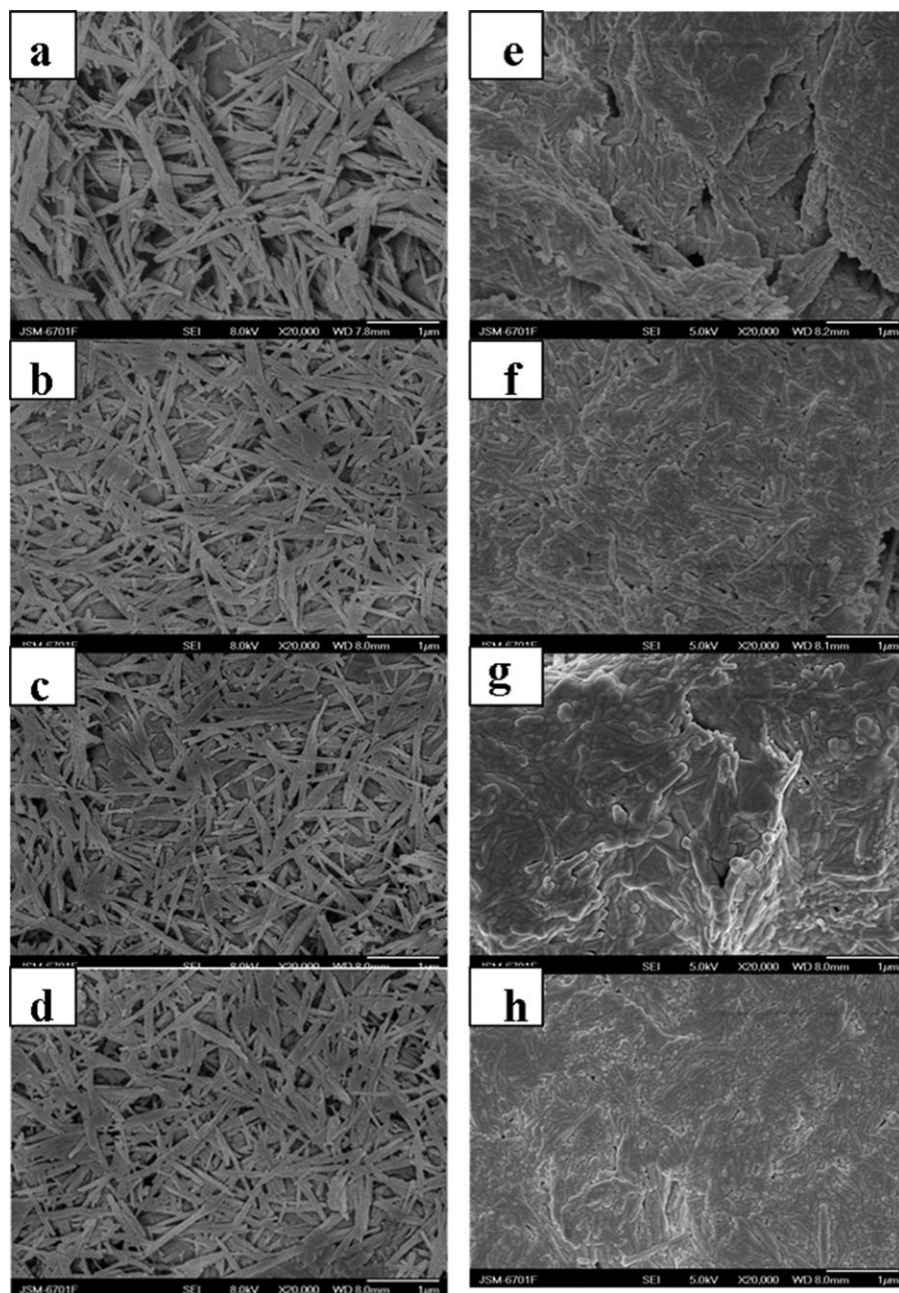**Figure 1.** FTIR spectra of (a) APT treated by water, (b) APT treated by $v(CH_3CH_2OH) : v(H_2O) = 5 : 5$ solution, (c) APT treated by ethanol, and (d–f) the corresponding superabsorbent nanocomposites.

and symmetric stretching vibrations of the ─COO⁻ groups, respectively. This reveals that AA monomers grafted on the backbones. The characteristic absorption of St cannot be obtained in FTIR spectra owing to the tiny amount of St in nanocomposite. The proof of the existence of St by UV–vis has been reported by the previous study.[33] In other words, the ethanol/water treatment has no influence on the structures of APT and superabsorbent nanocomposites, and the APT, AA, and St grafted onto the NaAlg backbones successfully.

SEM Analysis

FESEM photographs of the modified APT are observed and shown in Figure 2(a–d). The untreated APT crystal bundles [Figure 2(a)] were aggregated and only a few single rod-like crystals can be seen. In contrast, the APT crystal bundles [Figure 2(b)] treated by high-pressure homogenization process can be disaggregated effectively and the agglomerates were reduced evidently. The APT crystal bundles were disaggregated further with increasing the ethanol/water ratio [Figure 2(c)]. After treated by $v(CH_3CH_2OH) : (H_2O) - 5 : 5$ solution, the single rod-like crystals of the APT can be observed clearly. The excessive increase of ethanol/water ratio led to the reunite of some APT fibrous crystals [Figure 2(d)]. This phenomenon was caused by different properties of varying dispersion medium. Treated with the dispersion medium with low vapor pressure, high surface tension, and viscosity, APT clay tends to disaggregate easily during the homogenization.[35] Furthermore, relatively low surface tension of dispersion medium is benefit to reduce the reagglomeration of APT during drying process. As summarized in Table I, with the increasing ethanol/water ratio, the vapor pressure is increased, and the viscosity of dispersion medium first increases and then decreases. The change trend of viscosity is in accordance with the results about the dispersion state of APT clay. When $v(CH_3CH_2OH) < v(H_2O)$, the drying process is the main factor influencing the APT dispersion. The decreasing surface tension inhibited the reagglomeration of APT single crystals, and thus the APT crystal bundles were

Figure 2. SEM images of (a) untreated APT, (b) APT treated by water, (c) APT treated by $v(CH_3CH_2OH) : v(H_2O) = 5 : 5$ solution, (d) APT treated by ethanol, and (e–h) the corresponding superabsorbent nanocomposites.

Table I. The Vapor Pressure (P) and Viscosity (η) of Ethanol/Water Solution

$v(CH_3CH_2OH) : v(H_2O)$	P/kPa (25°C)	η/mPa·s
0 : 10	3.17	0.895
4 : 6	6.01	2.258
5 : 5	6.44	2.393
6 : 4	6.74	2.379
10 : 0	7.89	1.096

disaggregated better with increasing of ethanol/water volume ratio. However, when $v(CH_3CH_2OH) > v(H_2O)$, the homogenization process plays a dominate role. The increasing vapor pressure and the decreasing surface tension cause the agglomeration of APT. As a result, the optimal dispersion can be obtained at $v(CH_3CH_2OH) : v(H_2O) - 5 : 5$.

Figure 2(e, f) shows the surface morphology of the corresponding nanocomposites. The large aggregates are shown in Figure 2(e), containing untreated APT relative to the APT-treated samples [Figure 2(f, h)]. The nanocomposite [Figure 2(g)] containing APT-treated with $v(CH_3CH_2OH) : v(H_2O) - 5 : 5$ exhibited
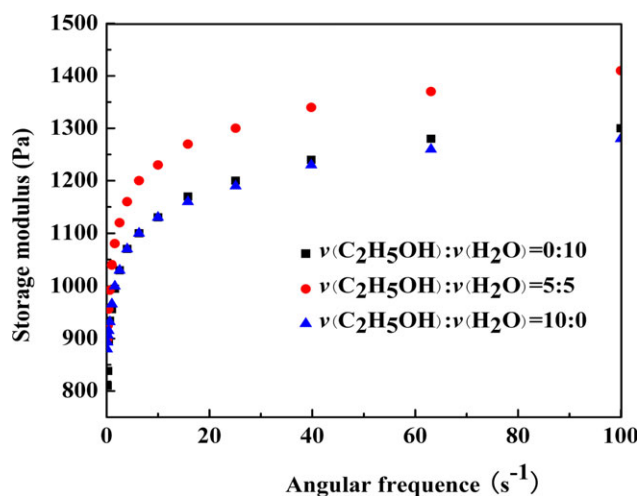
Figure 3. Effect of APT treated with different ethanol/water ratios on gel strength. [Color figure can be viewed in the online issue, which is available at wileyonlinelibrary.com.]

a rough and loose surface. The nanoscale APT rods were uniformly dispersed in the matrix. According to the FESEM observation, ethanol/water treatment of APT has great influence on the microstructure of the nanocomposite which was related to the swelling behaviors. Thus, the effect of different ethanol/water ratio dispersed APT on the swelling properties of the nanocomposite was investigated.

Gel Strength

The gel strengths of the superabsorbent nanocomposites were determined by a rheological method and denoted as a function of storage modulus (G') versus angular frequency (ω) (Figure 3). The result indicated that the G' values increased with an increase of ethanol/water ratio until an optimum was reached at the ratio of $v(CH_3CH_2OH) : v(H_2O) - 5 : 5$. The main reason is that the APT can act as crosslinking agent in the formation of three-dimensional network of the nanocomposite.[36] The better dispersion of APT, the more regular network can be formed, which could increase the strength of the gel network. Beyond to this ratio, the G' value of the nanocomposite decreased. This is because the agglomeration of APT makes the gel matrix discontinous, and thus the gel strength decreased.

Effect of Ethanol/Water Ratio on Water Absorbency and Swelling Rate

As shown in Figure 4, the water absorbency of NaAlg-g-P(NaA-co-St)/APT in distilled water and 0.9 wt % NaCl solutions increased with the increase of the ethanol/water ratio, reaching the maximum absorbency at $v(CH_3CH_2OH) : v(H_2O) - 5 : 5$ and then decreased. This can be attributed to the fact that the ethanol-assisted dispersion of APT during high-pressure homogenization can disperse APT bundles better than in aqueous solution. With the increase of the ethanol/water ratio, the APT crystal bundles can disaggregate effectively. The well disaggregation and dispersion of APT bundles into nanorod make more surface active —OH groups were exposed, and hence it can distribute in the three-dimensional network more even and form stronger bonding action with the polymer matrix. Thus, the
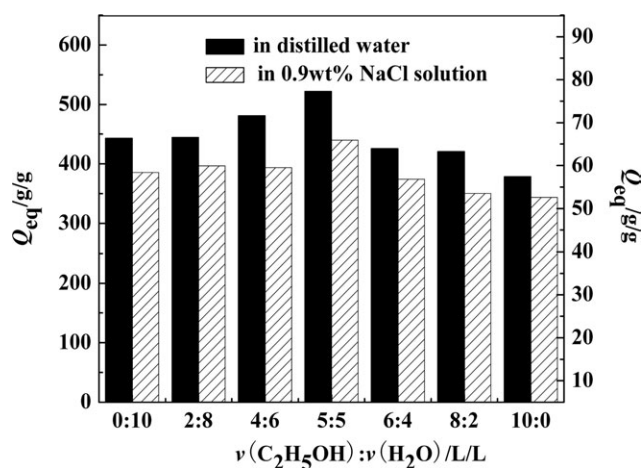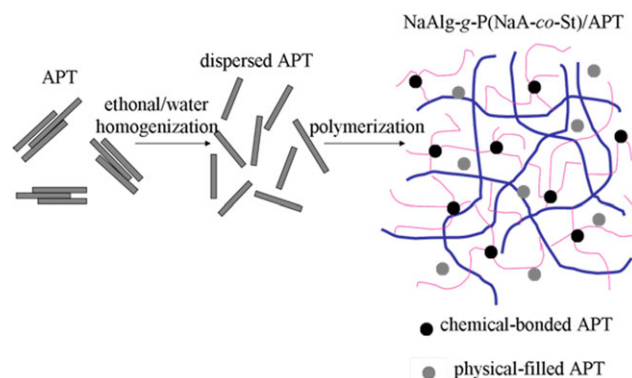

Figure 4. Effect of APT treated with different ethanol/water ratios on water absorbency.

water-holding network can be regularly formed under the "supporting" action of one-dimensional APT nanorod, and the water absorbent of the superabsorbent can be improved (Scheme 1). In addition, the APT that often acts as an inorganic crosslinker could disperse uniformly in NaAlg-g-P(NaA-co-St)/APT nanocomposite, which is benefit to form regular network structure and responsible for the enhancement of water absorbency. However, the higher ethanol/water volume ratio treatment often results in some aggregation of APT. The APT aggregation filled in the polymeric network, which was easy to block the absorption channels to restrain water movement. Thus, the water absorbency was decreased.
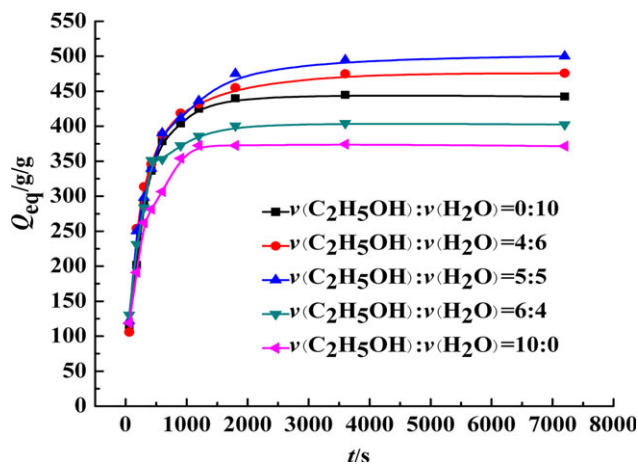
The effect of different ethanol/water ratio-treated APT on the swelling kinetics of the nanocomposites was also studied and shown in Figure 5. For the swelling kinetics analysis, the Schott's second-order swelling kinetics model can be used in this section[37]:

$$t/Q_t = 1/K_{is} + (1/Q)t \qquad (3)$$

where Q_t is the swelling ratio at time t; Q_∞ represents the theoretical equilibrium swelling ratio. On the basis of the
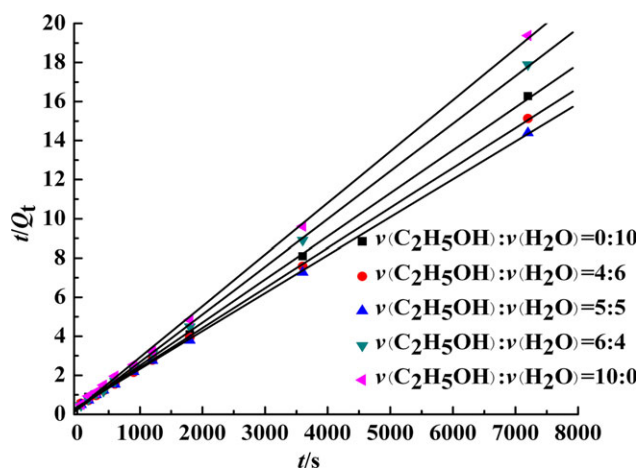

Scheme 1. Schematic illustration of the formation of (NaAlg-g-P(NaA-co-St)/APT) superabsorbent nanocomposite. [Color figure can be viewed in the online issue, which is available at wileyonlinelibrary.com.]

Figure 5. Effect of APT treated with different ethanol/water ratios on swelling rate. [Color figure can be viewed in the online issue, which is available at wileyonlinelibrary.com.]

experimental data, we can get an excellent straight line (Figure 6) with good linear correlation coefficients from the plots of t/Q_t against time t, indicating that the swelling of NaAlg-g-P(NaA-co-St)/APT nanocomposite acts in accordance with the second-order swelling kinetics. The values of the swelling kinetics obtained from Figure 6 are listed in Table II, suggesting that APT treated with moderate ethanol/water ratio brought a significant enhancement of the swelling rate as well as the initial swelling rate K_{is}. This is because the good dispersion of APT in the matrix could regulate the physical entanglement and the repulsion force of the macromolecule chains, which altered the network structure to increase the penetration and diffusion of water.[38] Thus, the swelling rate was increased. In a word, the ethanol/water-treated APT via high-pressure homogenization has a remarkable effect not only on water absorbency but also on swelling rate.

Figure 6. Swelling kinetics fitting curves of the superabsorbent nanocomposites introduced by APT treated with different ethanol/water ratios. [Color figure can be viewed in the online issue, which is available at wileyonlinelibrary.com.]

Table II. Swelling Kinetic Parameters for (NaAlg-g-P(NaA-co-St)/APT) Superabsorbent Nanocomposites Introduced the APT Treated with Different Ethanol/Water Ratios

$v(CH_3CH_2OH)$: $v(H_2O)$	Q_{eq} (g/g)	Q_∞ (g/g)	K_{is} (g/g/s)[a]	R[b]
0 : 10	442	454	3.3303	0.9996
4 : 6	481	490	3.9832	0.9999
5 : 5	521	515	4.5736	0.9999
6 : 4	425	409	4.2682	0.9998
10 : 0	378	380	3.5172	0.9996

[a]The initial swelling rate constant; (g/g)/s.
[b]Linear correlation coefficient.

Swelling and Deswelling Kinetics

The swelling kinetics of superabsorbent nanocomposites in different saline solutions (5 mmol/L) was investigated as shown in Figure 7. The change tendency of the swelling kinetics of the superabsorbent nanocomposite containing APT treated by different ethanol/water ratio was similar to that in distilled water. This agrees with the above views that the proper ethanol/water treatment can improve the dispersibility of APT in the matrix to alter the polymeric network for which the swelling rate can be increased in various saline solutions. As shown in Figure 7, it is found that the swelling behavior in $MgCl_2$ and $AlCl_3$ solution was different from that in NaCl solution. As the time increased, the water absorbency in $MgCl_2$ and $AlCl_3$ solution initially increased and then decreased. This can be attributed to that the multivalence cations in the polymeric network have high complexing ability to interact with $-COO^-$ of the polymer chains, which could increase the crosslink density and result in the expelling of the absorbed water.

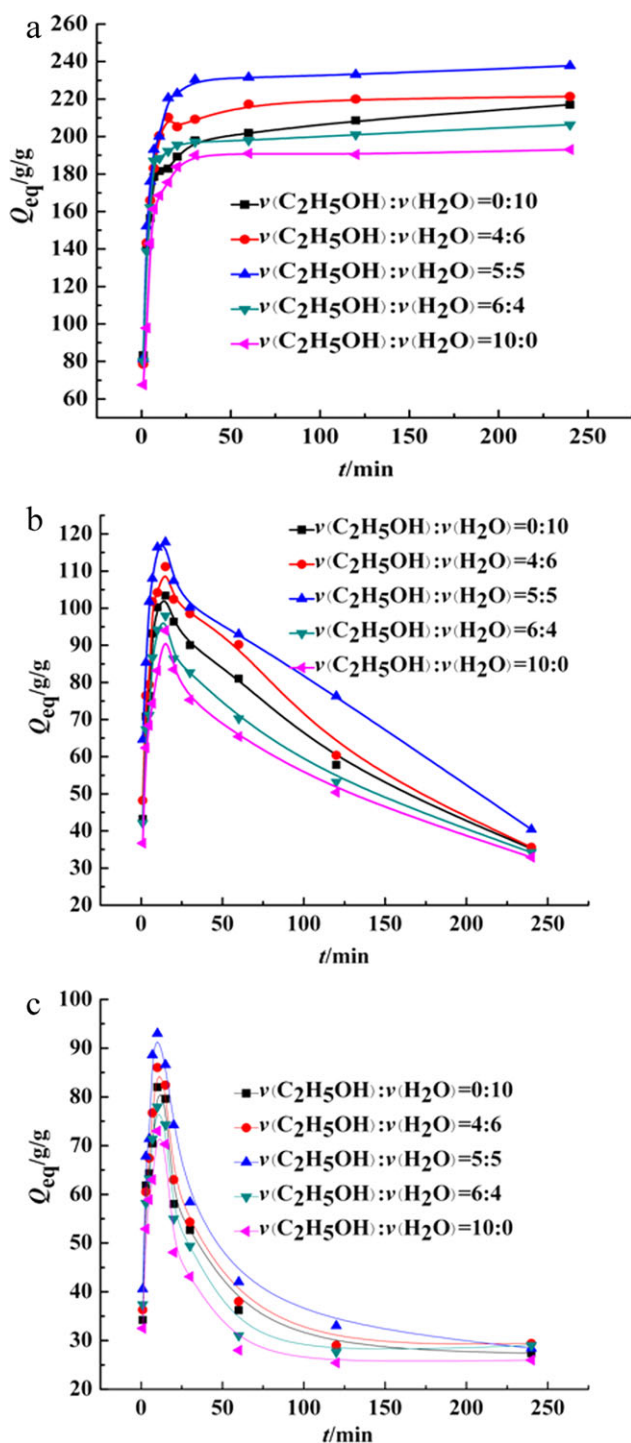To study the deswelling kinetics of the superabsorbent nanocomposites in NaCl, $MgCl_2$, and $AlCl_3$ solutions, the profiles of the water retention as a function dependent on the time t are shown in Figure 8. As it can be observed, the water retention was decreased quickly in the first second. This phenomenon can be explained by the fact that the osmotic pressure between gel network and external solution decreased and the polymer network sharply shrinked.[39] Moreover, it can be observed that the better dispersion of APT corresponds to a faster deswelling kinetics in this study. This is because that the uniform dispersion of the APT can provide water-release channels to break the skin layer.[40]

This fast swelling–deswelling behavior can further demonstrate that the good dispersion of APT improved the polymeric network greatly. Owing to the favorable elasticity of macromolecular chains in the relative regular network, the network can relax and shrink freely for which the movement of water molecules become fast. Thus, the nanocomposite containing APT treated with $v(CH_3CH_2OH)$: $v(H_2O) - 5 : 5$ solution has fast swelling–deswelling kinetics.

Reswelling Capability

Reswelling capability of a superabsorbent material is of great significance in many application fields such as agriculture and horticulture. Figure 9 shows the water absorbency curve for the
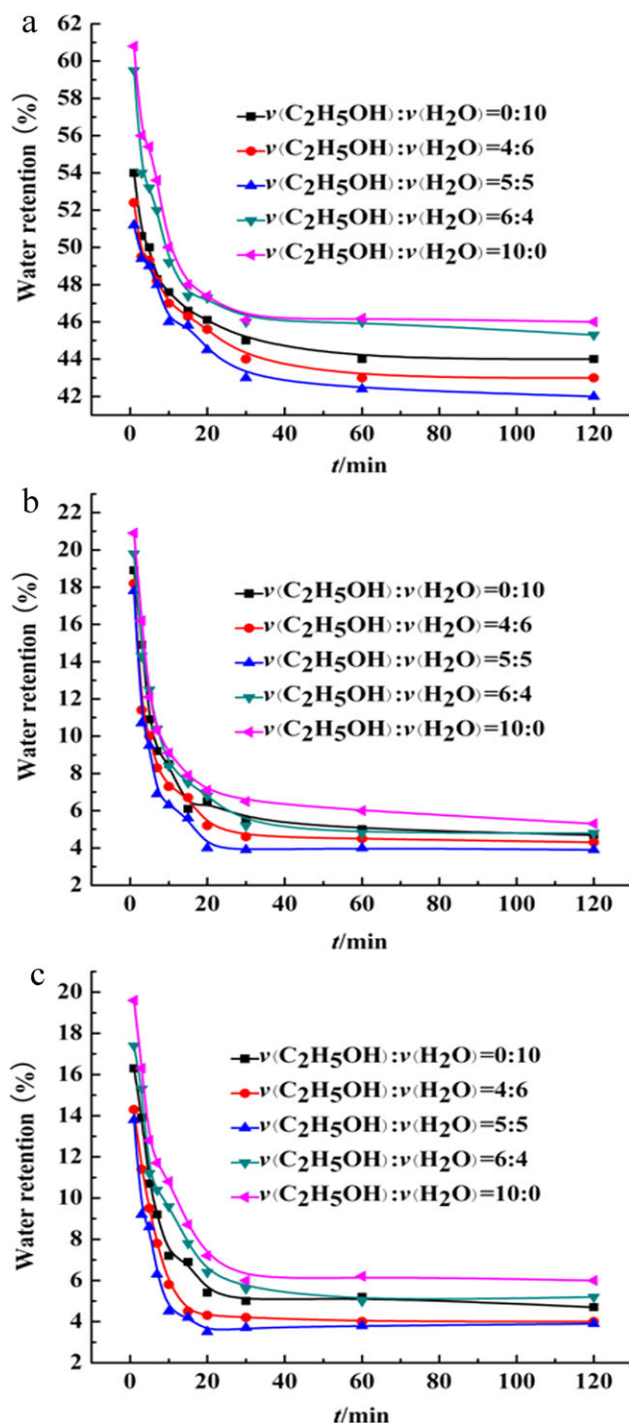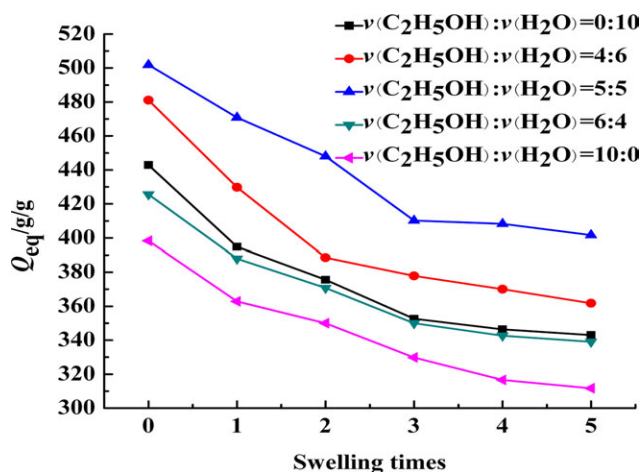
Figure 7. Swelling kinetics of the superabsorbent nanocomposites in (a) NaCl, (b) MgCl$_2$, and (c) AlCl$_3$ solution. [Color figure can be viewed in the online issue, which is available at wileyonlinelibrary.com.]

$v(CH_3CH_2OH) : v(H_2O) = 5 : 5$ solution reached 400 g/g after five reswelling times and the reswelling ability is better than other nanocomposites. This behavior can be attributed to the crosslinker role of the well-dispersed APT in the nanocomposite, which prevents the collapse of polymeric network structure during drying process. Thus, the decrease of water absorbency

Figure 8. Deswelling kinetics of the superabsorbent nanocomposites in (a) NaCl, (b) MgCl$_2$, and (c) AlCl$_3$ solution. [Color figure can be viewed in the online issue, which is available at wileyonlinelibrary.com.]

nanocomposites plotted against reswelling times. As it can be observed, each nanocomposite can retain certain degree of water absorption after several reswelling cycle, whereas the APT treated with different ethanol/water ratio has a big impact on reswelling ability of the nanocomposites. The water absorbency of the nanocomposite containing APT treated with

Figure 9. Effect of APT treated with different ethanol/water ratios on reswelling ability.[Color figure can be viewed in the online issue, which is available at wileyonlinelibrary.com.]

was not so evident with the increasing of reswelling times. This is in keeping with the result of gel strength analyzed above.

CONCLUSIONS

In this study, a series of ethanol/water-treated APT was introduced into the NaAlg-based superabsorbent network to study the effect of APT dispersion on the swelling properties of the nanocomposite. The FTIR and SEM analyses confirmed that the treatment can only disaggregate APT fibrous bundles and will not alter chemical structures. The improved dispersion of APT after treated by $v(CH_3CH_2OH) : v(H_2O) - 5 : 5$ solution resulted in the enhanced gel strength and swelling behavior (water absorbency, swelling rate, and reswelling ability) of the nanocomposite. In addition, the superabsorbent nanocomposite displayed fast swelling–deswelling performance in different salt solutions. Based on this study, it is concluded that the ethanol/water-treated clay via high-pressure homogenization had a good dispersion in the nanocomposite to better the polymeric network of the nanocomposite, which contributes to the improvement of the swelling properties.

ACKNOWLEDGMENTS

REFERENCES

1. Liu, M. Z.; Liang, R.; Zhan, F. L.; Liu, Z.; Niu, A. Z. *Polym. Int.* **2007**, *56*, 729.

2. Kosemund, K.; Schlatter, H.; Ochsenhirt, J. L.; Krause, E. L.; Marsman D. S.; Erasala, G. N. *Regul. Toxicol. Pharm.* **2008**, *53*, 81.

3. Atta, A. M.; Sayed, S. A.; Farag, A. B.; Ismails, S. H.; Mohamed, Z. M.; Eraky, A. M. *J. Disper. Sci. Technol.* **2011**, *32*, 1285.

4. Kaşgöz, H.; Durmus, A. *Polym. Adv. Technol.* **2008**, *19*, 838.

5. Wang, Q.; Wang, W. B.; Wu J.; Wang, A. Q. *J. Appl. Polym. Sci.* **2012**, *124*, 4424.

6. Hosseinzadeh, H. *J. Chem. Sci.* **2010**, *122*, 651.

7. Zhou, M.; Zhao, J. Z.; Zhou, L. Z. *J. Appl. Polym. Sci.* **2011**, *121*, 2406.

8. Urbano, B.; Rivas, B. L. *Polym. Int.* **2012**, *61*, 23.

9. Nakason, C.; Wohmang, T.; Kaesaman, A.; Kiatkamjornwong, S. *Carbohydr. Polym.* **2010**, *81*, 348.

10. Spagnol, C.; Rodrigues, F. H. A.; Pereira, A. G. B.; Fajardo, A. R.; Rubira, A. F.; Muniz, E. C. *Cellulose* **2012**, *19*, 1225.

11. Wang, W. B.; Wang Q.; Wang, A. Q. *Macromol. Res.* **2011**, *19*, 57.

12. Yang, S. P.; Fu, S. Y.; Liu, H.; Zhou, Y. M.; Li, X. Y. *J. Appl. Polym. Sci.* **2011**, *119*, 1204.

13. Liu, J. H.; Zhen, Y. A.; Wang, W. B.; Wang, A. Q. *J. Appl. Polym. Sci.* **2009**, *114*, 643.

14. Wang, W. B.; Zhai, N. H.; Wang, A. Q. *J. Appl. Polym. Sci.* **2011**, *119*, 3675.

15. Yang, J. S.; Xie, Y. J.; He, W. *Carbohydr. Polym.* **2011**, *84*, 33.

16. Pourjavadi, A.; Harzandi, A. M.; Hosseinzadeh, H. *Macromol. Res.* **2005**, *13*, 483.

17. Pourjavadi, A.; Hosseinzadeh, H.; Sadeghi, M. *J. Compos. Mater.* **2007**, *41*, 2057.

18. Lin, J. M.; Wu, J. H.; Yang, Z. F.; Pu, M. L. *Macromol. Rapid Commun.* **2001**, *22*, 422.

19. Xie, Y. T.; Wang, A. Q. *J. Compos. Mater.* **2009**, *43*, 2401.

20. Zhang, J. P.; Wang, Q.; Wang, A. Q. *Carbohydr. Polym.* **2007**, *68*, 367.

21. Zhen, Y. A.; Wang, A. Q. *J. Appl. Polym. Sci.* **2008**, *108*, 211.

22. Liu, J. H.; Wang A. Q. *J. Appl. Polym. Sci.* **2008**, *110*, 678.

23. Wang, W. B.; Wang, J.; Kang, Y. R.; Wang, A. Q. *Compos. B: Eng.* **2011**, *42*, 809.

24. Zhang, J. P.; Wang, A. Q. *React. Funct. Polym.* **2007**, *67*, 737.

25. Yadav, M.; Rhee, K. Y. *Carbohydr. Polym.* **2012**, *90*, 165.

26. Li, A.; Liu, R. F.; Wang, A. Q. *J. Appl. Polym. Sci.* **2005**, *98*, 1351.

27. Li, A.; Zhao, Y. G.; Wang, A. Q. *J. Appl. Polym. Sci.* **2007**, *105*, 3476.

28. Zhang, J. P.; Chen, H.; Li, P.; Wang, A. Q. *Macromol. Mater. Eng.* **2006**, *12*, 1529.

29. Wang, W. J.; Zhang, J. P.; Chen, H.; Wang, A. Q. *J. Appl. Polym. Sci.* **2007**, *103*, 2419.

30. Xu, J. X.; Zhang, J. P.; Wang, Q.; Wang, A. Q. *Appl. Clay Sci.* **2011**, *54*, 118.

31. Banchero, M.; Ferri, A.; Manna, L.; Sicardi, S. *Fluid Phase Equilibr.* **2006**, *243*, 107.

32. Chun, K. Y.; Choi, S. K.; Kang, H. J.; Park, C. Y.; Lee, C. J. *Carbon* **2006**, *44*, 1491.

33. Shi, X. N.; Wang, W. B.; Kang, Y. R.; Wang, A. Q. *J. Appl. Polym. Sci.* **2012**, *125*, 1822.

34. Ramazani-Harandi, M. J.; Zohuriaan-Mehr, M. J.; Yousefi, A. A.; Ershad-Langroudi A.; Kabiri, K. *Polym. Test* **2006**, *25*, 470.

35. Cheng, Q. H.; Debnath, S.; Gregan, E.; Byrne, H. J. *J. Phys. Chem. C* **2010**, *114*, 8821.

36. Haraguchi, K.; Takehisa, T.; Fan, S. *Macromolecules* **2002**, *35*, 10162.

37. Schott, H. *J. Macromol. Sci. B: Phys.* **1992**, *31*, 1.

38. Omidian, H.; Hashemi, S. A.; Sammes, P. G.; Meldrum, I.; *Polymer* **1999**, *40*, 1753.

39. Buchanan, K. J.; Hird, B.; Letcher, T. M. *Polym. Bull* **1986**, *15*, 325.

40. Lee, W. F.; Fu, Y. T. *J. Appl. Polym. Sci.* **2003**, *89*, 3652.